(12) **UK Patent Application** (19) **GB** (11) **2 441 787** (13) **A**

(43) Date of A Publication **19.03.2008**

(21) Application No: **0618240.6**

(22) Date of Filing: **15.09.2006**

(71) Applicant(s):
ElectroMagnetic GeoServices AS
(Incorporated in Norway)
Stiklestadveien 1, N-7041 Trondheim, Norway

(72) Inventor(s):
Rune Mitter
Odd Marius Aakervik

(74) Agent and/or Address for Service:
Kilburn & Strode
20 Red Lion Street, LONDON, WC1R 4PJ, United Kingdom

(51) INT CL:
G01B 7/30 (2006.01) *G01C 15/00* (2006.01)
G01V 3/00 (2006.01) *G01V 3/12* (2006.01)

(52) UK CL (Edition X):
G1N NACNN NCSA N19B2A N3S7 N7T1A

(56) Documents Cited:
GB 2415511 A **GB 2413188 A**
GB 2413187 A **GB 2220070 A**
GB 2197078 A **GB 1342475 A**
FR 002586302 A1 **US 4396885 A**
US 20040176910 A

(58) Field of Search:
UK CL (Edition X) **G1N**
INT CL **G01B, G01C, G01R, G01V**
Other: **online: WPI, EPODOC**

(54) Abstract Title: **Method of determining the orientation of an electric and magnetic receiver deployed remotely**

(57) A method of determining the orientation of an electric and magnetic receiver deployed remotely which comprises: measuring electric and magnetic data in response to an applied active source; resolving the data into components in-line (x-component) to the electric dipole of the receiver and orthogonal to this (y-component); the data is transformed from the time domain to the frequency domain and normalised; and the rotation angle 0 between the direction of the source dipole and the receiver dipole is calculated. The invention is suitable for determining the orientation of receivers which have been deployed for use in a sub-sea survey. A claim is included for a method of approximating absolute phase measurements which comprises: Measuring electric and magnetic data in response to an applied active source; Resolving the data into components in-line (x-component) to the electric dipole of the receiver and orthogonal to this (y-component); the data is transformed from the time domain to the frequency domain and normalised; identifying the minimum horizontal offset between source and receiver; comparing at all frequencies the phase at this minimum offset with a pre calculated phase for zero offset obtained from forward modelling; and calculating an average time difference to be applied to measure data to approximate absolute phase measurement.

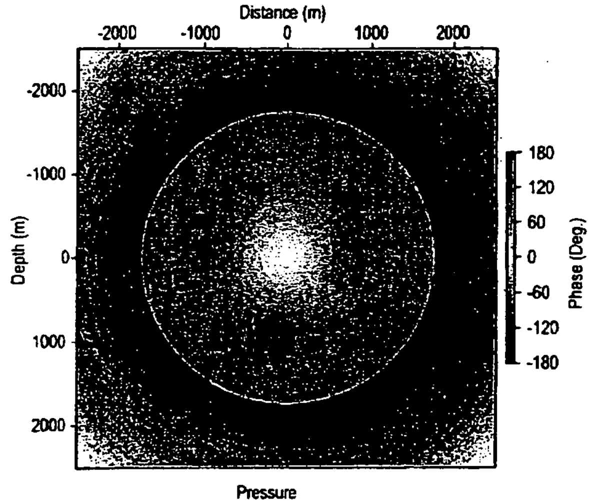

FIG. 3

GB 2 441 787 A

At least one drawing originally filed was informal and the print reproduced here is taken from a later filed formal copy.

Original Printed on Recycled Paper

This is a reprint to rectify errors introduced in the course of reproduction–Second Search Report printed–27.03.2008

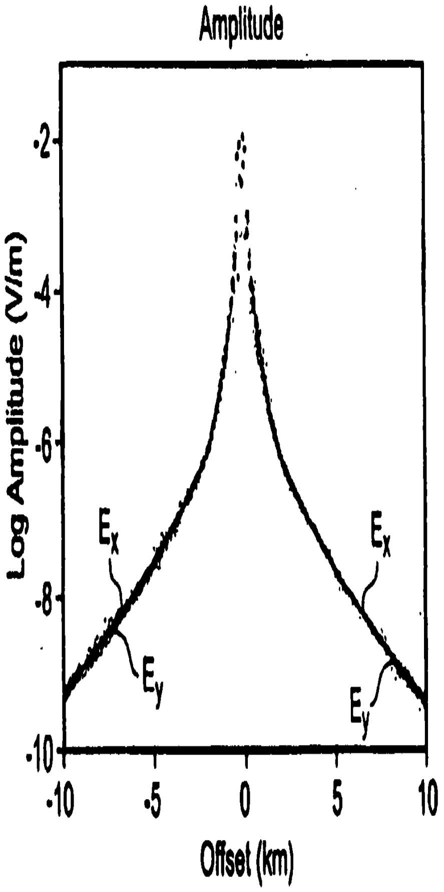
Amplitude
Log Amplitude (V/m)
-2
-4
-6
-8
-10
E_x
E_y
E_x
E_y
-10
-5
0
5
10
Offset (km)

FIG. 1A

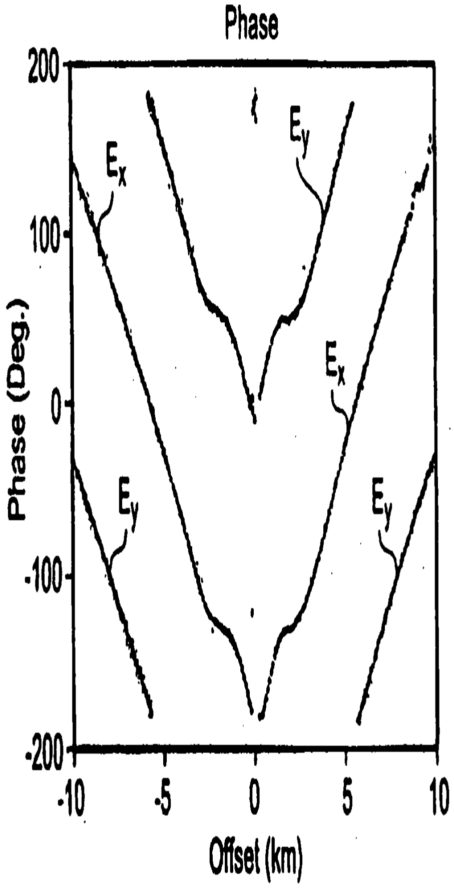
Phase
Phase (Deg.)
200
100
0
-100
-200
E_x
E_y
E_x
E_y
E_y
-10
-5
0
5
10
Offset (km)

FIG. 1B

26 09 07

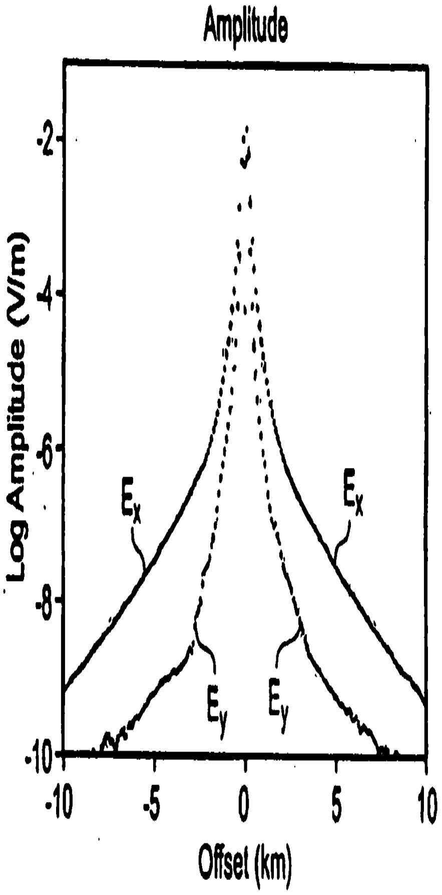

FIG. 2A

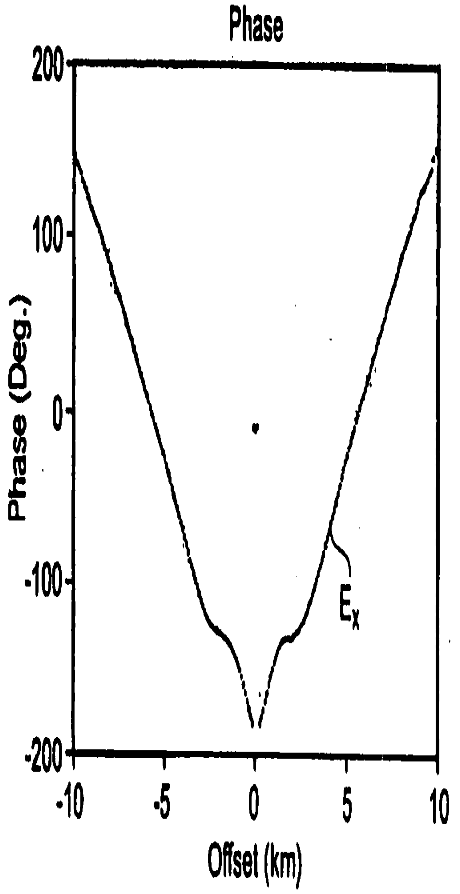

FIG. 2B

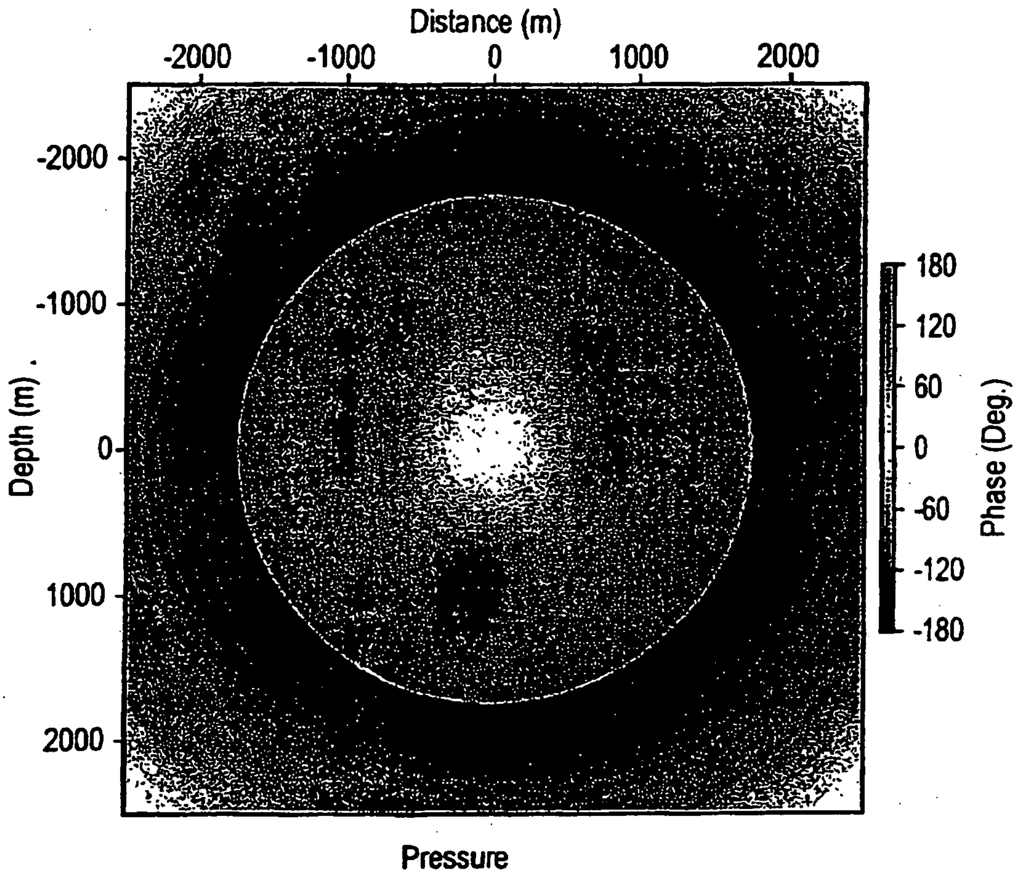
Distance (m)
-2000
-1000
0
1000
2000
Depth (m)
-2000
-1000
0
1000
2000
180
120
60
0
-60
-120
-180
Phase (Deg.)
Pressure

FIG. 3

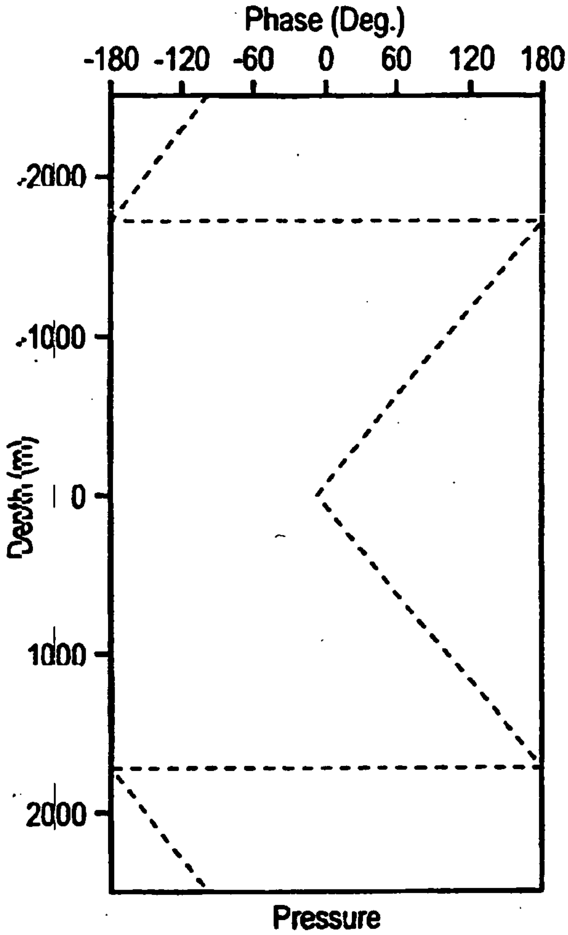
Phase (Deg.)
-180 -120 -60 0 60 120 180
-2000
-1000
Depth (m)
0
1000
2000
Pressure

FIG. 4

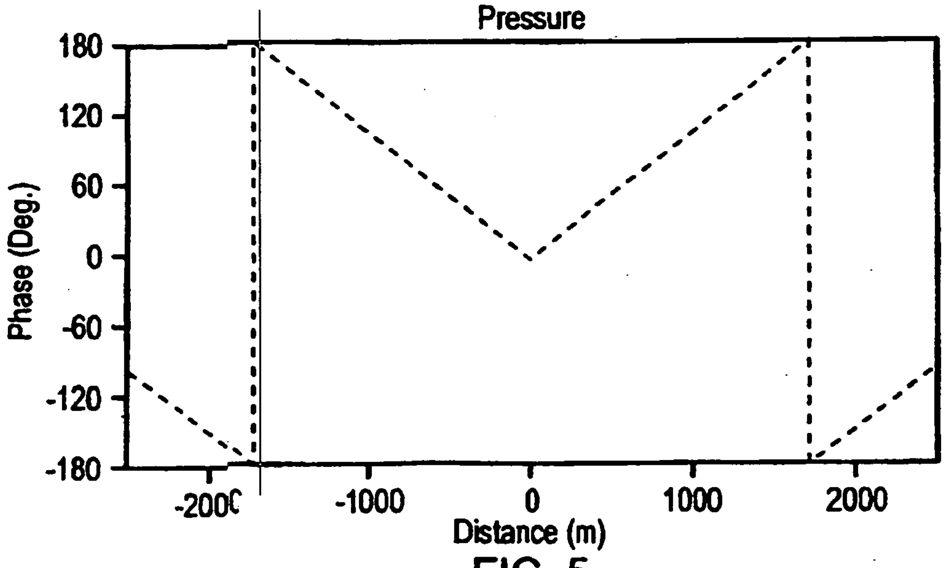
Pressure
180
120
60
0
-60
-120
-180
Phase (Deg.)
-2000 -1000 0 1000 2000
Distance (m)

FIG. 5

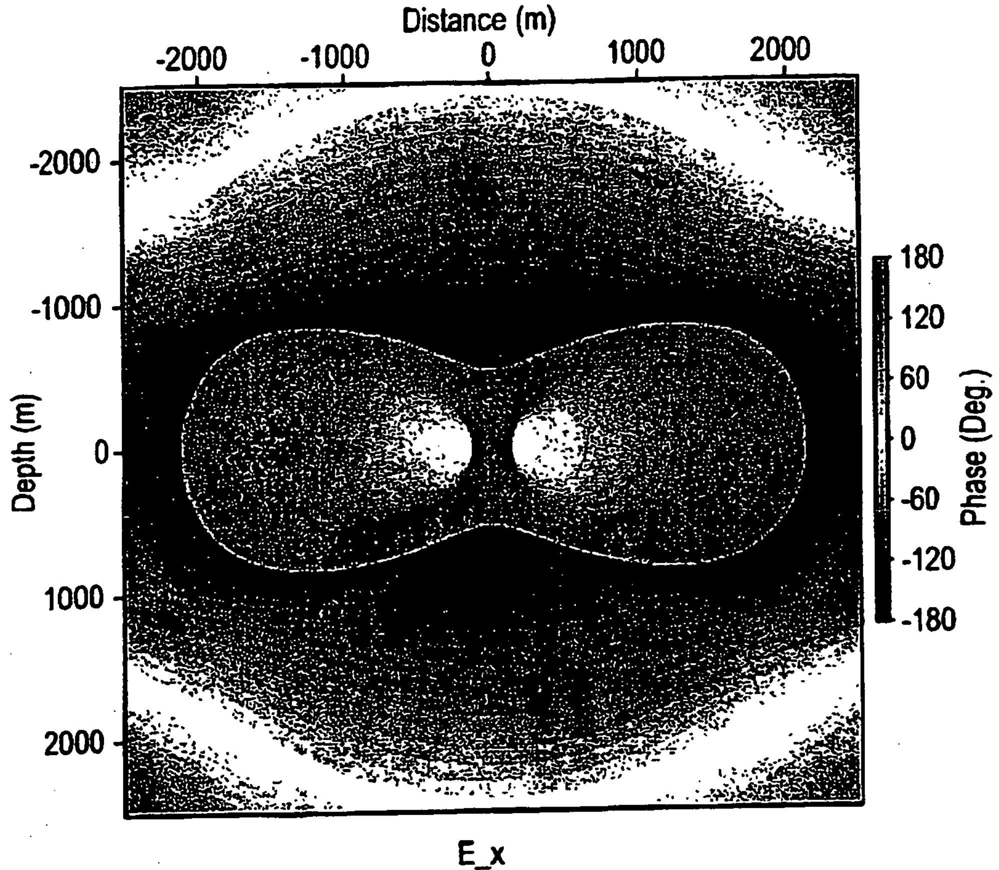
Distance (m)
-2000
-1000
0
1000
2000
Depth (m)
-2000
-1000
0
1000
2000
180
120
60
0
-60
-120
-180
Phase (Deg.)
E_x

FIG. 6

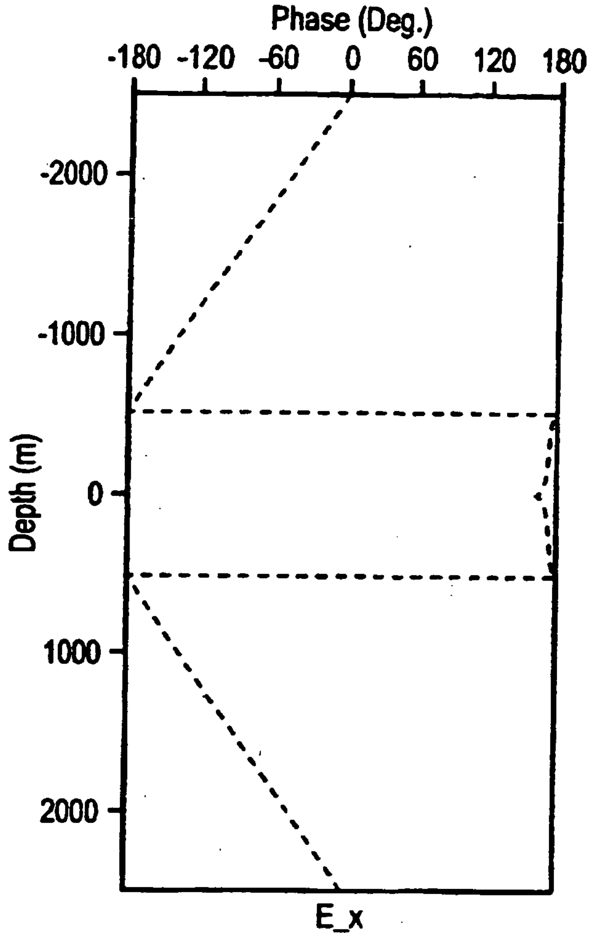
Phase (Deg.)
-180 -120 -60 0 60 120 180
Depth (m)
-2000
-1000
0
1000
2000
E_x

FIG. 7

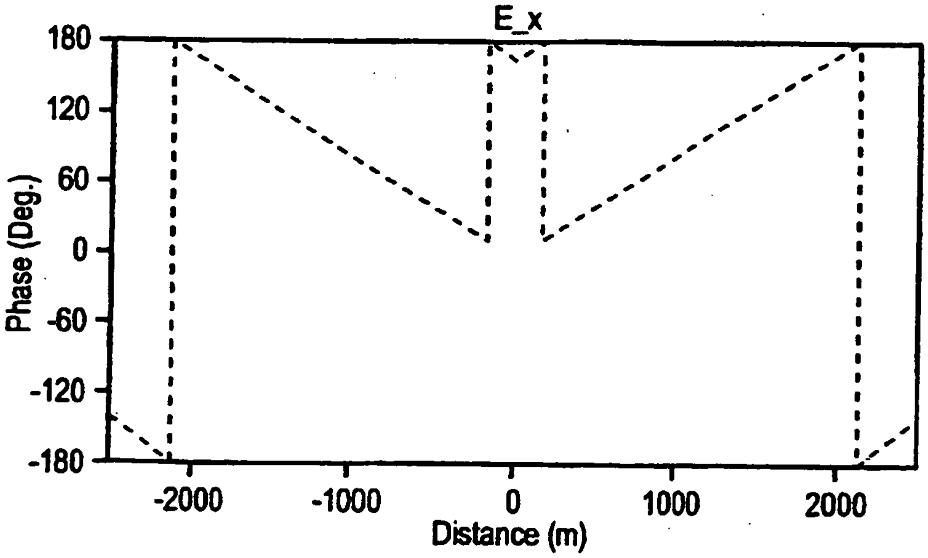
E_x
Phase (Deg.)
180
120
60
0
-60
-120
-180
-2000 -1000 0 1000 2000
Distance (m)

FIG. 8

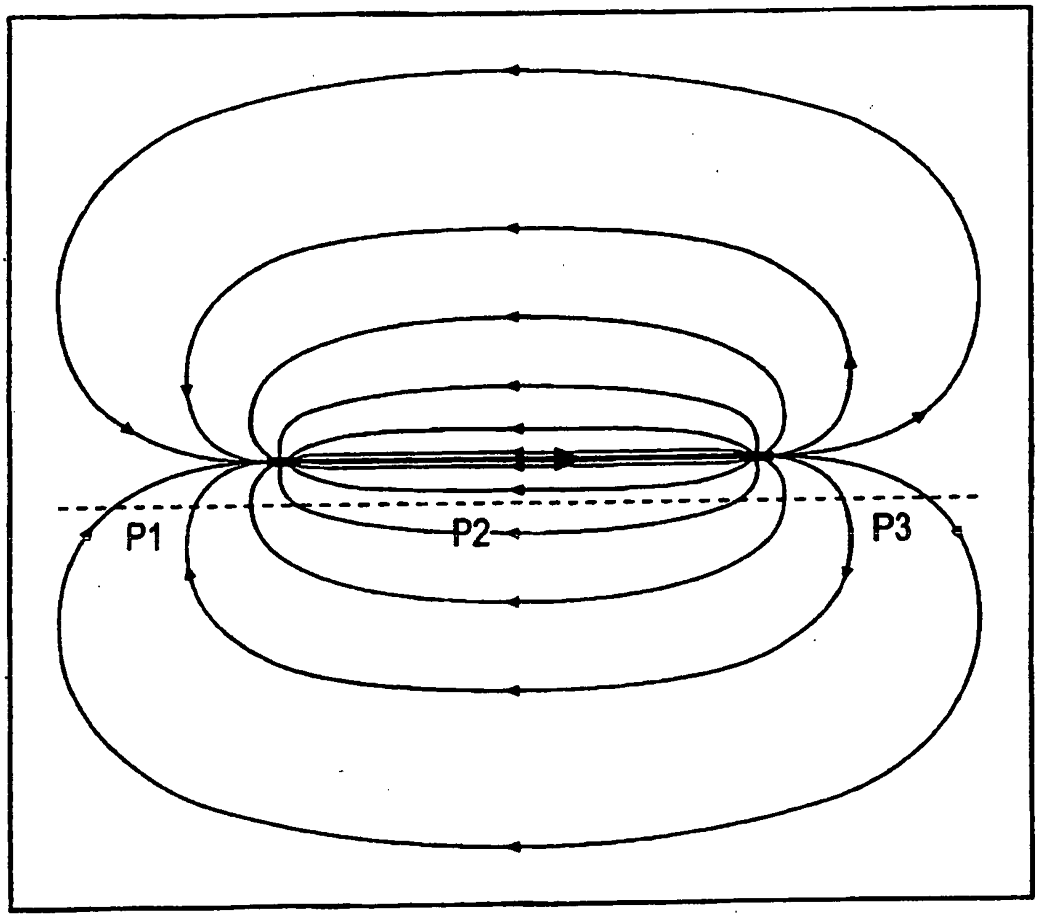

FIG. 9

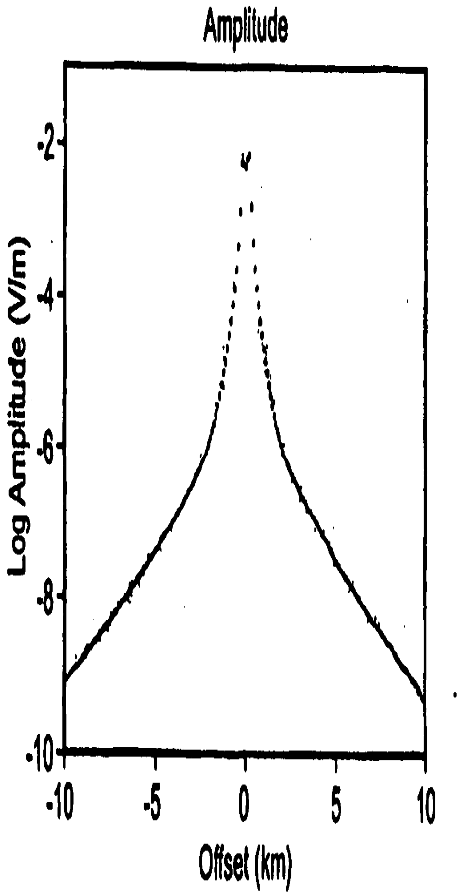

FIG. 10A

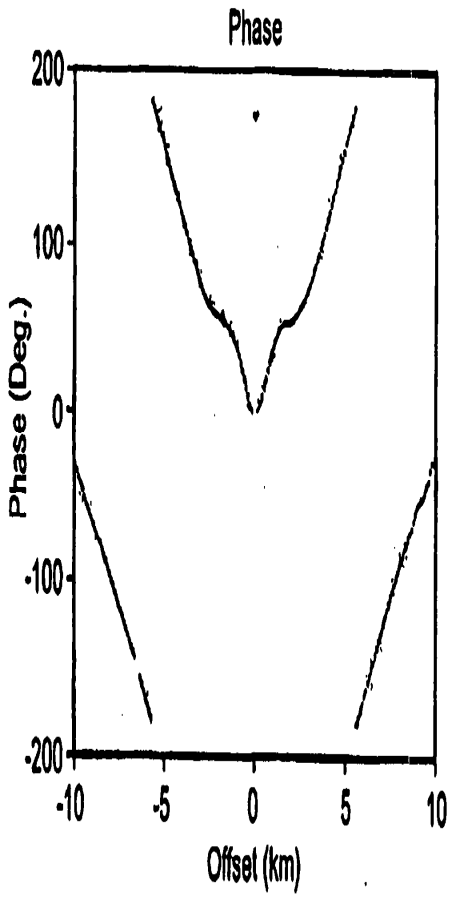

FIG. 10B

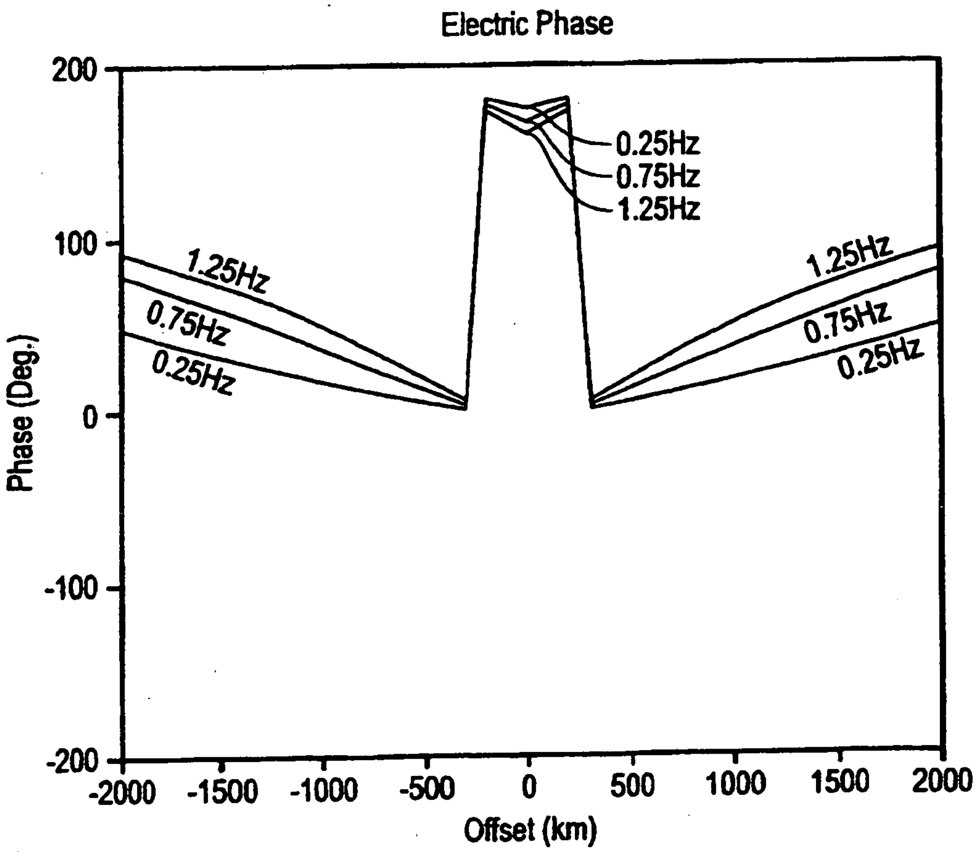

Electric Phase
200
100
0
-100
-200
Phase (Deg.)
-2000
-1500
-1000
-500
0
500
1000
1500
2000
Offset (km)
0.25Hz
0.75Hz
1.25Hz
1.25Hz
0.75Hz
0.25Hz
1.25Hz
0.75Hz
0.25Hz

FIG. 11

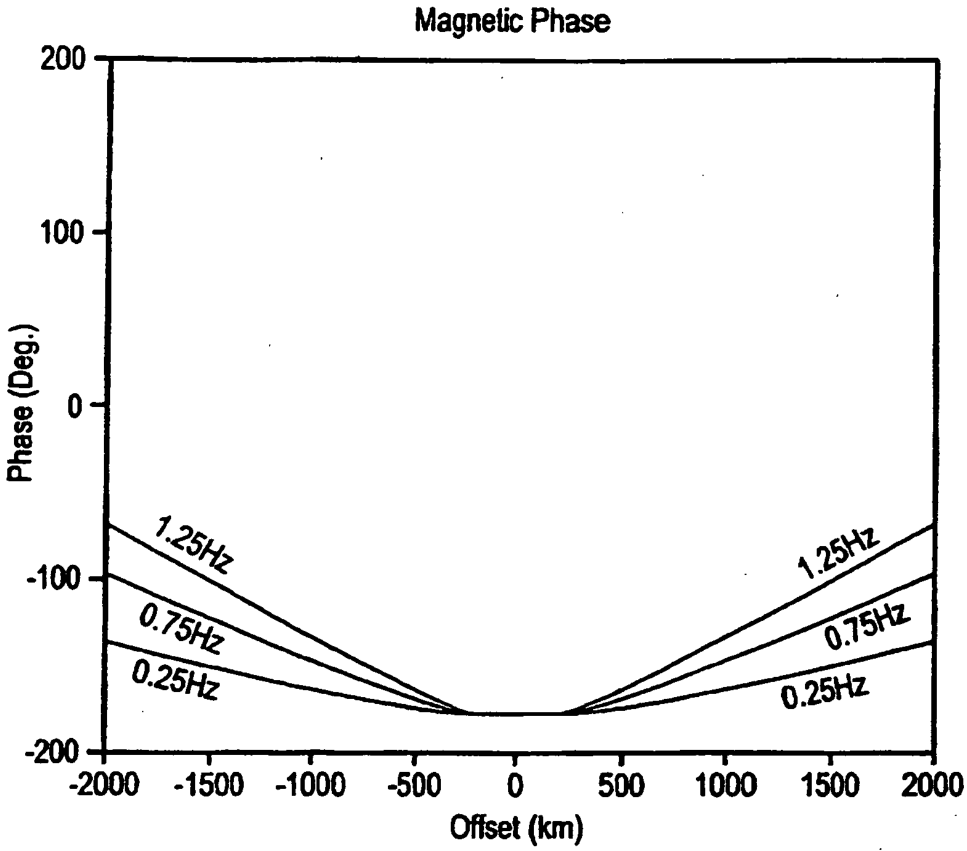
Magnetic Phase
200
100
0
-100
-200
Phase (Deg.)
1.25Hz
0.75Hz
0.25Hz
1.25Hz
0.75Hz
0.25Hz
-2000
-1500
-1000
-500
0
500
1000
1500
2000
Offset (km)

FIG. 12

2441787

Receiver orientation

The present invention relates to a method for determining the orientation of receivers which have been deployed for use in a sub sea survey, in particular for use in an electromagnetic (EM) survey.

Controlled Source Electromagnetic (CSEM) surveying methods for the direct detection of hydrocarbons (also known as Sea Bed Logging (SBL)) uses an active EM source to probe the underground for thin, high resistive layers. Hydrocarbon filled reservoirs will typically have a resistivity that is of one to two orders of magnitude higher than a water filled reservoir and the surrounding shale or mud rock. This difference is sufficient to support a partially guided or ducted field in the reservoir which will subsequently leak energy up to EM field receivers placed on the seabed.

The SBL experiment consists of dropping electric and magnetic sensors onto the seabed along a predetermined sail line and subsequently towing a horizontal electric dipole source along this line. The sail line starts at approximately 10 km before the first receiver and ends at approximately 10 km after the last receiver. Thus, all receivers have at least active source data with source receiver offsets of 10 km. During deployment, the receivers will spin around their respective vertical axes on the way from the vessel at the sea surface to the seabed and therefore they have an arbitrary orientation when they reach the seabed.

One means for measuring this orientation of the receiver of the seabed is using a gyroscope. There are a number of reasons for this not being a standard and these include the cost of a sufficiently accurate gyroscope and the energy consumption. Gyroscopes which have the level of accuracy required for SBL surveys are expensive and for some surveys it will be necessary to deploy 100 or more receivers in a grid on the seabed. The cost of obtaining and maintaining a gyroscope for each receiver is prohibitive. When they are used they have high energy consumption. This therefore requires larger battery packages and leads to increased weight of the receivers. This is an unwanted side effect.

Compasses are another possible solution for orientation measurements. They are standard equipment on the receivers, but they have accuracy problems. Compasses must be carefully calibrated when placed on a receiver which carries electric equipment and has a number of metal surfaces. For example, if the battery package is changed, then the compass must be recalibrated. This means a recalibration of the compass for each drop of each receiver. This is not a trivial procedure on board the survey vessel where again you may be deploying in excess of 100 receivers for a survey. Re-calibration may therefore not take place as often as it should and receiver orientation may not be sufficiently well determined, if the receivers have only compass measurements.

It is therefore an object of the present invention to determine receiver orientation once deployed from field data measured at the receiver in order that the presence or absence of a resistive body can be determined from receiver measurements.

According to a first aspect of the present invention there is provided a method of determining the orientation of an electric and magnetic receiver deployed remotely which comprises: measuring electric and magnetic data in response to an applied active source; resolving the data into components in-line (x-component) to the electric dipole of the receiver and orthogonal to this (y-component); the data is transformed from the time domain to the frequency domain and normalised; and the rotation angle θ between the direction of the source dipole and the receiver dipole is calculated.

Comparing towing the EM transmitter over a resistive body versus a conductive body, one of the characteristic responses of the resistive layer is an increased amplitude in the measured electric field. Data from a receiver with a towline over a generally conductive formation can be chosen as a reference. An anomaly can be identified by normalizing the amplitude for each receiver using the reference dataset. Relative amplitudes that are large compared to unity may indicate a resistive body in the subsurface. However, the depth of the resistive body can not be found with this qualitative technique. In order to find the depth to a resistive body, the absolute phase must also be known.

The depth of a resistive body can be found either by depth migration or inversion techniques. Both types of methods require absolute phase data. Measurement of absolute phase require accurate time measurements and in particular that the clock time stamping the transmitter current is synchronized with the clock time stamping the receiver data. There is information in the combined measurement of transmitter current and receiver data that make it possible to do a quality control of this synchronization. However, problems may occur if the synchronization of clocks is lost and measurement of absolute phase is difficult.

It is therefore a further object of the present invention to provide a means for approximating absolute phase measurements in order to determine the depth of any resistive body detected.

According to a second aspect of the present invention, there is provided a method of approximating absolute phase measurements which comprises: : measuring electric and magnetic data in response to an applied active source; resolving the data into components in-line (x-component) to the electric dipole of the receiver and orthogonal to this (y-component); transforming the data from the time domain to the frequency domain; identifying the minimum horizontal offset between source and receiver; comparing at all frequencies the phase at this minimum offset with a pre calculated phase for zero offset obtained from forward modelling; and calculating an average time difference to be applied to measured data to approximate absolute phase measurement.

The data measured by the receivers may be normalised with reference to the phase of the transmitter signal. Alternatively, it may be further normalised with reference to the absolute value of the dipole moment.

The wavefield is preferably applied by means of a transmitter located at or near the seabed and may be at a frequency between 0.01 and 20Hz. The EM wavefield may be transmitted at a number of discrete frequencies to allow a range of measurements to be taken. The EM wavefield may be transmitted at a wavelength between 1S and 50S, where S is the thickness of the overburden above the considered strata.

The invention may be carried into practice in various ways and one approach to the determination of the orientation of a deployed receiver and an approximation of the absolute phase from the receiver will now be described in detail. This is by way of example in order to illustrate the calculation.

Spatial Rotation

The two horizontal electric components measured at the receiver are $e_x(x_r|x_s,\omega)$ and $e_y(x_r|x_s,\omega)$, with x_r the receiver position, x_s the source position and ω angular frequency. The towline is chosen to be our desired x-direction. This will also be referred to as the inline direction. The receivers are dropped to the sea bed and in general the receiver's x-direction will not coincide with the towline direction. However, the measured components can be rotated so that the new x-direction along the dipole axis of the receiver coincides with the towline direction.

The two horizontal electric components in the coordinate system where the x-direction coincide with the towline direction is $E_x(x_r|x_s,\omega)$ and $E_y(x_r|x_s,\omega)$. Thus,

$$\begin{aligned} E_x(x_r|x_s,\omega) &= e_x(x_r|x_s,\omega)\cos(\theta) - e_y(x_r|x_s,\omega)\sin(\theta), \\ E_y(x_r|x_s,\omega) &= e_x(x_r|x_s,\omega)\sin(\theta) + e_y(x_r|x_s,\omega)\cos(\theta) \end{aligned} \tag{1}$$

and,

$$\begin{aligned} e_x(x_r|x_s,\omega) &= E_x(x_r|x_s,\omega)\cos(\theta) + E_y(x_r|x_s,\omega)\sin(\theta), \\ e_y(x_r|x_s,\omega) &= -E_x(x_r|x_s,\omega)\sin(\theta) + E_y(x_r|x_s,\omega)\cos(\theta). \end{aligned} \tag{2}$$

The rotation angle θ should ideally be measured, but an approximation can be found from the data. The approximation is good if the transmitter points in the direction of the towline and the earth locally is well described by a plane layer geometry. In this case the electric field normal to the towline should be close to zero, and we should have a minimum in this electric component,

$$E_y(x_r|x_s,\omega) = e_x(x_r|x_s,\omega)\sin(\theta) + e_y(x_r|x_s,\omega)\cos(\theta) \tag{3}$$

Alternatively, for the same configuration, there should be a minimum in the inline magnetic field,

$$H_x(x_r|x_s,\omega) = h_x(x_r|x_s,\omega)\cos(\theta) - h_y(x_r|x_s,\omega)\sin(\theta) \quad (4)$$

and a maximum for the cross line magnetic field,

$$H_y(x_r|x_s,\omega) = h_x(x_r|x_s,\omega)\sin(\theta) + h_y(x_r|x_s,\omega)\cos(\theta). \quad (5)$$

The derivation to follow is for the electric field. The derivation for the magnetic field is then trivial. In order to determine the rotation angle θ, we minimize the expression,

$$\mathcal{E}_E = \sum_{x_s}\sum_{\omega} W(x_r|x_s,\omega)E_y(x_r|x_s,\omega)E_y^*(x_r|x_s,\omega) \quad (6)$$

or

$$\varepsilon_E = \sum_{x_s}\sum_{\omega} W(x_r|x_s,\omega)(e_x(x_r|x_s,\omega)\sin(\theta)+e_y(x_r|x_s,\omega)\cos(\theta)) \\ (e_x(x_r|x_s,\omega)\sin(\theta)+e_y(x_r|x_s,\omega)\cos(\theta))^* \quad (7)$$

For magnetic data the alternative is to minimize $H_x(x_r|x_s,\omega)$ in equation (4). To simplify the formalism we define the partial sums,

$$\Gamma_{xx} = \sum_{x_s}\sum_{\omega} W(x_r|x_s,\omega)e_x(x_r|x_s,\omega)e_x^*(x_r|x_s,\omega)$$
$$\Gamma_{xy} = \sum_{x_s}\sum_{\omega} W(x_r|x_s,\omega)\frac{1}{2}(e_x(x_r|x_s,\omega)e_y^*(x_rA|x_s,\omega)+e_x^*(x_r|x_s,\omega)e_y(x_r|x_s,\omega))$$
$$\Gamma_{yy} = \sum_{x_s}\sum_{\omega} W(x_r|x_s,\omega)e_y(x_r|x_s,\omega)e_y^*(x_r|x_s,\omega) \quad (8)$$

Equation (7) is then expressed,

$$\varepsilon_E = \Gamma_{xx}\sin^2(\theta) + 2\Gamma_{xy}\sin(\theta)\cos(\theta) + \Gamma_{yy}\cos^2(\theta) \quad (9)$$

An extremum in $E_y(x_r|x_s,\omega)$ requires,

$$\delta_\theta \epsilon_E = 0$$

(10)

And the requirement of this extremum being a minimum is

$$\delta_\theta^2 \varepsilon_E > 0$$

(11)

The rotation angle that minimises $E_y(x_r|x_s, \omega)$ is given by

$$\tan(2\theta) = \frac{-2\Gamma_{xy}}{\Gamma_{xx} - \Gamma_{yy}}$$

(12)

In the case of a positive second derivative in equation (11), that is if

$$(\Gamma_{xx} - \Gamma_{yy})\cos(2\theta) - 2\Gamma_{xy}\sin(2\theta) > 0$$

(13)

If the second derivative in equation (11) is negative, then we are at a maximum for $E_y(x_r|x_s, \omega)$ and the minimum is at $\theta = \pm\pi/2$ if θ is measured in radians or $\theta = \pm 90$ if θ is measured in degrees. Whether to use plus or minus does not matter. The reason is that the prescribed method minimize $E_y(x_r|x_s, \omega)$. There are two possible solution to a minimum in $E_y(x_r|x_s, \omega)$. The desired solution is when $E_x(x_r|x_s, \omega)$ point in the positive towline direction. The other possible outcome is when $E_x(x_r|x_s, \omega)$ point in the negative towline direction. In order to discriminate between these two solutions, additional information must be used. This information is possible to retrieve from the data if the transmitter current data is analyzed in combination with the receiver data.

Absolute Phase

A realistic analysis of the electromagnetic field close to an electric dipole in sea water, relevant for SBL data, must be performed with both an air layer above and a formation below the transmitter. This is the procedure followed when QC or correction tables used for processing are built.

However, for pedagogical reasons we discuss the problem of a horizontal electric dipole in sea water first. For distances up to some hundred meters from the transmitter this model is sufficiently close to the realistic case.

Let ϵ_0 be the electric permittivity of vacuum with ϵ the relative permittivity. The conductivity is σ. The complex electric permittivity is then,

$$\tilde{\varepsilon} = \varepsilon\varepsilon_0 + i\frac{\sigma}{\omega} \tag{14}$$

With μ the magnetic permeability, the complex wavenumber is determined by,

$$k_\omega^2 = \mu\tilde{\varepsilon}\omega^2 \tag{15}$$

Introducing the magnetic vector potential by,

$$B(x \mid x_s) = \nabla \mathrm{x} A(x \mid x_s) \tag{16}$$

The equation for the magnetic vector potential in a homogeneous medium can be expressed

$$\nabla^2 A(x \mid x_s) + k_\omega^2 A(x \mid x_s) = -\mu J(x_s) \tag{17}$$

where $J(x_s)$ is the source-current density. The electric field is given by the electric scalar potential, $\Phi(x|x_s)$, and the magnetic vector potential as,

$$E(x \mid x_s) = -\nabla\Phi(x \mid x_s) + i\omega A(x \mid x_s) \tag{18}$$

The scalar and vector potentials satisfy the Lorenz gauge condition,

$$\nabla \cdot A(x \mid x_s) = i\omega\mu\tilde{\varepsilon}\Phi(x \mid x_s) \tag{19}$$

which give,

$$\Phi(x|x_s) = \frac{-1}{i\omega\mu\tilde{\varepsilon}} \nabla \cdot A(x|x_s) \tag{20}$$

With the Lorenz gauge condition, the electric field in equation (18), can be expressed in terms of the vector potential only,

$$E(x|x_s) = i\omega \left\{ \frac{1}{k_\omega^2} \nabla(\nabla \cdot A(x|x_s)) + A(x|x_s) \right\} \tag{21}$$

Each component of the vector potential in equation (17), satisfy an equation of the form,

$$\nabla^2 g_0(x|x_s) + k_\omega^2 g_0(x|x_s) = -\delta(x - x_s) \tag{22}$$

where $g_0(x|x_s)$ is a scalar Green's function. With the relative distance, R, given by,

$$R = |x - x_s| \tag{23}$$

the scalar Green's function is,

$$g_0(x|x_s) = \frac{e^{ik_\omega R}}{4\pi R} \tag{24}$$

We further introduce the auxiliary quantity $a(k_\omega R)$,

$$a(k_\omega R) = \frac{i}{k_\omega R} - \frac{1}{(k_\omega R)^2} \tag{25}$$

and by using equation (21), we can define the electric Green's tensor for an electric dipole source,

$$G_{mn}^{EJ}(x|x_s) = i\omega\mu \left\{ (1 + a(k_\omega R))\delta_{mn} - (1 + 3a(k_\omega R)) \frac{x_m x_n}{R^2} \right\} g_0(x|x_s)$$

(26)

such that the electric field is given by

$$E_m(x) = \int dx_s G_{mn}^{EJ}(x \mid x_s) J_n(x_s)$$

(27)

The electric field due to a realistic electric dipole source can be found by an integral over infinitesimal electric dipole source elements.

For comparison, the acoustic field from a seismic source array with notional source signature distribution $S(x_s)$ is,

$$P(x) = \int dx_s g_0(x \mid x_s) S(x_s)$$

(28)

The present invention is further exemplified with reference to the following figures in which:

Figure 1 shows measured field data prior to inline rotation with figure 1a showing the amplitudes of measured fields and figure 1b showing phase of the measured fields;

Figure 2 shows measured field data after inline rotation with figure 2a showing amplitude and figure 2b showing phase;

Figure 3 shows the distribution of phase for the acoustic field in an x-z cross section through the source plane;

Figure 4 shows a depth trace through the source location from figure 3;

Figure 5 shows a trace in the x-direction from figure 3 at a distance of 10m below the source location;

Figure 6 shows the distribution of phase for the electric inline field in an x-z cross section through the source plane;

Figure 7 shows a depth trace through the source location from figure 6;

Figure 8 shows a trace in the x-direction from figure 6 at a distance of 10m below the source location;

Figure 9 shows the radiation pattern for a horizontal electric dipole (HED);
Figure 10 shows measured field data after inline rotation and final 180 degree correction with figure 10a showing amplitude and figure 10b showing phase;
Figure 11 shows modelled inline electric data due to a 220 m long HED and R_0 = 30 m for frequencies of 0.25Hz, 0.75Hz and 1.25Hz; and
Figure 12 shows modelled cross line magnetic data due to a 220 m long HED and R_0 = 30 m for frequencies of 0.25Hz, 0.75Hz and 1.25Hz.

Results

The measured electric and magnetic data are normally transformed from the time domain to the frequency domain. The desired source receiver offsets are specified. From the navigation data you can find the time corresponding to each source receiver offset. The signal is extracted for some periods around these central times and these traces are transformed to the frequency domain. The actual number of periods will naturally depend on the base frequency for the survey. Traces with the same time intervals are extracted from the transmitter signal.

The electric and magnetic data are then normalized by the phase of the transmitter signal. The result is electric data measured in V/m and magnetic data measured in A/m with absolute phase. Alternatively, the electric and magnetic data can further be normalized with the absolute value of the dipole moment which is electric current times dipole length.

Figure 1a shows the amplitudes of the measured horizontal electric fields. Both the E_x component and the E_y component. The source receiver offsets are from -10 km to 10 km. The amplitudes of the two components are of equal size and the traces therefore lie on top of each other. Thus, in this case the receiver has landed on the seabed with an orientation that relative to the towline is ±45 degrees or ±135 degrees.

Figure 1b shows the phases of the horizontal electric fields. The two components are shifted 180 degrees with respect to each other. A 180 degrees phase shift is the same as a difference in sign. The reason for the difference in sign is that one component is oriented in the positive towline direction and one component is oriented in the negative towline direction. If the receiver is oriented at -45 degrees or +135 degrees, then both components should have the same sign. At -45 degrees orientation both E_x and E_y point in the positive towline direction. At +135 degrees orientation both E_x and E_y point in the negative towline direction. Thus, this receiver must point in either the +45 degrees direction or in the -135 degrees orientation. How to resolve the true orientation direction is discussed below.

Figure 2a shows the amplitudes of the horizontal electric fields after the inline rotation angle is found from equations (12) and (13) and the application of this angle in equation (1). The E_y component is now close to two orders of magnitude smaller than the E_x component. The actual rotation angle in this case is +44 degrees or alternatively -136 degrees. Thus, after rotation, the E_x component in Figure 2a is either 0 degrees or ±180 degrees with respect to the towline direction.

Figure 2b shows the phase of the inline horizontal electric field (E_x). It is this curve that will be used to resolve the final problem of determining the true orientation. The procedure used here concentrates on the minimum source receiver separation. The reason is that propagation effects are minimal when the source receiver separation is minimal. It is then important to analyse and understand electric and magnetic phase for this configuration.

You look first at the phase of the electric field due to an electric dipole before the corresponding phase of the magnetic field. For comparison you may first have a closer look at the simpler phase behaviour of the acoustic field in equation (28).

The Green's function $g_0(x|x_s)$ is valid for a homogeneous acoustic medium. Figure 3 show the distribution of the phase in the x and z plane. The source location is (0,0,0). The cross section is in the source plane. The x-axis is denoted "distance" and the z-axis is denoted "depth". For an acoustic field, the wavenumber is real and we have,

$$k_\omega = \frac{\omega}{c_{ph}} \tag{29}$$

where, for the example in Figure 3, the phase velocity, c_{ph} is 866 m/s and the frequency is 0.25 Hz. This particular phase velocity value is chosen for comparison with the electric field in seawater at the same frequency. In Figure 3 we see that the phase starts out at 0 and it increase linearly with distance from the source in all directions.

Figure 4 is a trace in the depth direction from Figure 3. The x-position is 0. Figure 5 is a trace in the x-direction from Figure 3. The depth is 10 m below the source location. The linear increase with distance is evident in both Figure 4 and Figure 5. If the depth is further increased for the trace in the x-direction, a hyperbolic move out would be evident. The linear increase in phase with offset reflects the constant phase velocity. The phase, ϕ, is given directly by

$$\phi = \frac{\omega R}{c_{ph}}$$

A temporal Fourier transform of $g_0(x|x_s)$ give,

$$g_0(x,t\,|\,x_s,0) = \frac{\delta(t - \frac{R}{c_{ph}})}{4\pi R} \tag{30}$$

Thus, Figure 3 can be interpreted as a travel time map for the acoustic field. It is also clear that when the phase velocity increases, the gradient in phase with respect to source receiver offset decreases since the gradient is inversely proportional to the phase velocity. If the phase velocity becomes very high, the gradient in phase with respect to source receiver offset goes to zero over a distance of 10 km. If the phase map is interpreted as a travel time map, the small gradient reflects the fact that at high velocity it takes little time to travel to the largest offset.

Figure 6 show the phase of the inline electric field for the same cross section as the acoustic field in Figure 3. The frequency is 0.25 Hz and the conductivity is 3.33 S/m. The inline electric field is given by equation (27), and is due to an electric dipole of length 270 m. This phase distribution is clearly different from that of the acoustic field. Figure 7 is a trace in the depth direction from Figure 6. The x-position is 0. Figure 8 is a trace in the x-direction from Figure 6. The depth is 10 m below the source location.

The electric field has strong near field effects. This is apparent in Figure 7 where we see that the phase gradient is very small the first 500 meters away from the source location. This indicates a large phase velocity in this area. The electric field appears nearly instantaneous here, even if we are in a strongly conductive medium. At larger offsets the gradient approaches the same value as for the acoustic field. The reason is that the electric far field for the given conductivity model and frequency has the same phase velocity as for the acoustic field in Figures 3 - 5.

The appearance of the electric field along the x-direction is different, and does not show similar strong near field effects. However, by comparing figure 8 with the acoustic phase in Figure 5, it is clear that the wrap around from + 180 degrees to -180 degrees happens at a larger offset for the electric field. This indicates a larger average phase velocity for the electromagnetic field at small source-receiver offsets. Note that with the given parameters, the acoustic field in Figure 3 and the electric field in Figure 6 will have the same phase velocity in the far field region.

Another interesting and important observation from Figure 8 (but also apparent in Figures 6 and 7) is that the phase is not zero close to the source. It is close to 180 degrees here. If the transmitter is an infinitesimal horizontal electric dipole (very short HED), this phase is close to 180 degrees is a good approximation. In our case we used a HED of length 270 m. The deviation from 180 degrees is due to the final length of the transmitter dipole. The phase at zero offset (minimum source receiver separation) is 162 degrees in the given example.

At zero offset in Figure 8 the observation (receiver) location are 10 meters below the centre of the transmitter. If the transmitter runs a current in the positive x-direction, then the return current in the sea water must be in the negative x-direction at this location. This is the reason for the close to 180 degrees phase shift. This is illustrated in Figure 9, where the source current is from left to right which is also the positive x-direction. The return current immediately below the transmitter, at position P2, is pointing in the opposite direction. This is also the local direction of the inline electric field. So if the electric dipole current points in the positive x-direction, the inline electric field at position P2 will point in the negative x-direction.

If we move to a location immediately in front of the transmitter, at position P3 in Figure 9, or immediately behind the receiver, at position P1 in Figure 9, we observe from Figure 8 that the phase drop to slightly more than zero degrees. The inline electric field is here in phase with the source current. From Figure 9 we see that this is in accordance with the radiation pattern of an electric dipole in a conducting medium. For larger offsets the phase increase with distance.

The fact that the electric current in seawater, immediately below the transmitter, must be close to 180 degrees out of phase with the transmitter, can be used at the final stage of the receiver rotation procedure described above. Going back to the inline electric field in Figure 2, we observe that the phase at zero offset does not compare well with the inline electric field in Figure 8. The receiver in Figure 2 is oriented along the negative inline direction. This can be fixed by multiplying the field in Figure 2 with -1. This does not change the amplitude but give a 180 degrees spatial rotation. The result is shown in Figure 10.

The phase is shown in Figure 10b. The phase is now close to 180 degrees at zero offset and dropping to close to zero degrees in front of and behind the transmitter. The phase gradient is smaller on the real data in Figure 10b than for the synthetic data in Figure 8. The reason is that for the synthetic data we used a model with seawater only. The real data is influenced by propagation of the electric field in a formation that has a lower conductivity than seawater. However, when source receiver separations are very small, the direct field in seawater dominate the response and the assumption of a close to 180 degrees phase rotation is still valid for zero or minimum offset.

A proper analysis of the electric near field for an SBL experiment requires that the effect of formation and air layer is included. In this case analytical expressions are no longer available, but extensive modelling studies can be used to build up sufficient information. An example of the electric inline component, $E_x(x_r|x_s,\omega)$, for a realistic formation is shown in Figure 11. The transmitter length is 220 m.

Three frequencies are shown in this case, that is 0.25 Hz, 0.75 Hz and 1.25 Hz. From Figure 11 it is clear that the zero offset inline electric phase is frequency dependent. The 0.25 Hz zero offset phase is 175 degrees. The 0.75 Hz zero offset phase is 166 degrees. The 1.25 Hz zero offset phase is 159 degrees. It turns out that the most important parameters determining this zero offset phase are transmitter length, L, distance from transmitter centre to receiver, R_0, angular frequency, ω, and seawater conductivity, σ_w. All these quantities are measured in an SBL survey.

For marine environments, the zero or minimum offset phase is much less sensitive to top formation conductivity and total water depth. If the source is not towed directly above the receiver, a true horizontal zero offset can not be realized. However, a minimum horizontal offset can still be found. The smallest R_0 value will be for this minimum horizontal offset. It is the total distance between the centre of the transmitter and the receiver that is important for the phase properties. This distance can be obtained from navigation since the source elevation is measured. In the following we will refer to the minimum horizontal offset also as zero offset.

If the synchronization between transmitter clock and receiver clock is lost for some reason, then there is a possibility to recover from this failure by close inspection of the electric data at zero offset. The procedure requires a four dimensional table to be pre calculated by forward modelling. This table must contain absolute phase as a function of transmitter length, distance from the transmitter centre to receiver, frequency and seawater conductivity. By comparing the zero offset phases for all frequencies of the inline real data with the tabulated value, a single, averaged, time delay or time advance, $\Delta\tau$, may be deduced. Assume that the measured zero offset phase for the inline electric component is $\phi_{Ex}(\omega)$ and the tabulated inline zero offset phase is $\phi_{TAB}(\omega,L,R_0,\sigma_w)$. Then,

$$\omega\Delta\tau = \phi_{E_x}(\omega) - \phi_{TAB}(\omega, L, R_0, \sigma_w) \tag{31}$$

If n_ω, frequencies are available, one possible averaging procedure is,

$$\Delta\tau = \frac{1}{n_\omega}\sum_\omega \frac{\phi_{E_x}(\omega) - \phi_{TAB}(\omega, L, R_0, \sigma_w)}{\omega} \tag{32}$$

Figure 12 show the phase of the cross line magnetic field, $H_y(x_r|x_s,\omega)$. The formation, frequencies and transmitter length is the same as for the inline electric field in Figure 11. From Figure 12 it is clear that the zero offset cross line magnetic phase is much less frequency dependent than the zero offset inline electric phase. The 0.25 Hz zero offset phase is -179.5 degrees. The 0.75 Hz zero offset phase is -178.8 degrees. The 1.25 Hz zero offset phase is -178.1 degrees. In general, the zero offset cross line magnetic phase show much less variation with transmitter length, distance from the transmitter centre to receiver, frequency and seawater conductivity than the zero offset electric phase.

As for the zero offset electric phase, the zero offset magnetic phase is not very sensitive to top formation conductivity and total water depth. The largest effects on the zero offset cross line magnetic phase can be observed when the frequency is above 1 Hz and the distance from the transmitter centre to receiver is more than 100 m. In this case the zero offset magnetic phase can be -170 degrees to -160 degrees. For frequencies less than 1 Hz and R0 less than 100 m, the zero offset magnetic phase, is usually between -180 degrees and -175 degrees.

Claims

1. A method of determining the orientation of an electric and magnetic receiver deployed remotely which comprises: measuring electric and magnetic data in response to an applied active source; resolving the data into components in-line (x-component) to the electric dipole of the receiver and orthogonal to this (y-component); the data is transformed from the time domain to the frequency domain and normalised; and the rotation angle θ between the direction of the source dipole and the receiver dipole is calculated.

2. A method as claimed in Claim 1, in which the data is normalised with reference to the phase of the transmitter signal.

3. A method as claimed in Claim 2, in which the data is further normalised with reference to the absolute value of the dipole moment.

4. A method as claimed in any preceding Claim, in which the EM field is applied by means of a transmitter located at or near the seabed.

5. A method as claimed in any preceding Claim, in which the EM wavefield is transmitted at a frequency between 0.01 and 20Hz.

6. A method as claimed in any preceding Claim, in which the EM wavefield is transmitted at a number of discrete frequencies.

7. A method as claimed in any preceding Claim, in which the EM wavefield is transmitted at a wavelength between 1S and 50S, where S is the thickness of the overburden above the considered strata.

8. A method of approximating absolute phase measurements which comprises: : measuring electric and magnetic data in response to an applied active source; resolving the data into components in-line (x-component) to the electric dipole of the receiver and orthogonal to this (y-component); the data is transformed from the time domain to the frequency domain and normalised; identifying the minimum horizontal offset between source and receiver; comparing at all frequencies the phase at this minimum offset with a pre calculated phase for zero offset obtained from forward modelling; and calculating an average time difference to be applied to measured data to approximate absolute phase measurement.

9. A method as claimed in Claim 8, in which the data is normalised with reference to the phase of the transmitter signal.

10. A method as claimed in Claim 9, in which the data is further normalised with reference to the absolute value of the dipole moment.

11. A method as claimed in any of Claims 8 to 10, in which the EM field is applied by means of a transmitter located at or near the seabed.

12. A method as claimed in any of Claims 9 to 12, in which the EM wavefield is transmitted at a frequency between 0.01 and 20Hz.

13. A method as claimed in any of Claims 9 to 13, in which the EM wavefield is transmitted at a number of discrete frequencies.

14. A method as claimed in any of Claims 9 to 14, in which the EM wavefield is transmitted at a wavelength between 1S and 50S, where S is the thickness of the overburden above the considered strata.

Application No: GB0618240.6 **Examiner:** Mr Daniel Jones

Claims searched: 1-7 **Date of search:** 22 January 2007

Patents Act 1977: Search Report under Section 17

Documents considered to be relevant:

Category	Relevant to claims	Identity of document and passage or figure of particular relevance
X	1 at least.	FR 2586302 A1 (COMMISSARIAT A L'ENERGIE ATOMIQUE) Most of document is relevant, see also page 8 lines 23-27.
A	-	GB 2220070 A (RADIODETECTION LTD.) See abstract.
A	-	GB 1342475 A (ANTHONY WILLIAM RUSSELL)
A	-	GB 2197078 A (RADIODETECTION LTD.)
A	-	US 4396885 A (CONSTANT)

Categories:

X	Document indicating lack of novelty or inventive step	A	Document indicating technological background and/or state of the art.
Y	Document indicating lack of inventive step if combined with one or more other documents of same category.	P	Document published on or after the declared priority date but before the filing date of this invention.
&	Member of the same patent family	E	Patent document published on or after, but with priority date earlier than, the filing date of this application.

Field of Search:

Search of GB, EP, WO & US patent documents classified in the following areas of the UKC^{X} :

G1N

Worldwide search of patent documents classified in the following areas of the IPC

G01B; G01C; G01R; G01V

The following online and other databases have been used in the preparation of this search report

WPI, EPODOC

Application No: GB0618240.6 **Examiner:** Mr Daniel Jones

Claims searched: 8-14 **Date of search:** 22 March 2007

Patents Act 1977
Further Search Report under Section 17

Documents considered to be relevant:

Category	Relevant to claims	Identity of document and passage or figure of particular relevance
A	-	GB 2413187 A (ELECTROMAGNETIC GEOSERVICES AS)
A	-	US 2004/176910 A (STATOIL ASA)
A	-	GB 2413188 A (ELECTROMAGNETIC GEOSERVICES AS)
A	-	GB 2415511 A (STATOIL ASA, ELECTROMAGNETIC GEOSERVICES AS)

Categories:

X	Document indicating lack of novelty or inventive step	A	Document indicating technological background and/or state of the art.
Y	Document indicating lack of inventive step if combined with one or more other documents of same category.	P	Document published on or after the declared priority date but before the filing date of this invention.
&	Member of the same patent family	E	Patent document published on or after, but with priority date earlier than, the filing date of this application.

Field of Search:

Search of GB, EP, WO & US patent documents classified in the following areas of the UKC^{X} :

G1N

Worldwide search of patent documents classified in the following areas of the IPC

G01B; G01R; G01V

The following online and other databases have been used in the preparation of this search report

WPI, EPODOC